Copy 44
RM SL56C19
0.2

NACA

RESEARCH MEMORANDUM

for the

Bureau of Aeronautics, Department of the Navy

MINIMUM DRAG OF THE CHANCE VOUGHT XF8U-1 AIRPLANE AS DETERMINED FROM THE FLIGHT TEST OF A 0.11-SCALE ROCKET-BOOSTED MODEL AT MACH NUMBERS BETWEEN 0.73 AND 1.71

TED NO. NACA DE 392

By Earl C. Hastings, Jr.

Langley Aeronautical Laboratory
Langley Field, Va.

NATIONAL ADVISORY COMMITTEE
FOR AERONAUTICS

WASHINGTON

NATIONAL ADVISORY COMMITTEE FOR AERONAUTICS

RESEARCH MEMORANDUM

for the

Bureau of Aeronautics, Department of the Navy

MINIMUM DRAG OF THE CHANCE VOUGHT XF8U-1 AIRPLANE AS DETERMINED FROM THE FLIGHT TEST OF A 0.11-SCALE ROCKET-BOOSTED MODEL AT MACH NUMBERS BETWEEN 0.73 AND 1.71

TED NO. NACA DE 392

By Earl C. Hastings, Jr.

SUMMARY

Drag data obtained from the flight of a 0.11-scale rocket-boosted model of the Chance Vought XF8U-1 airplane are presented herein. The Mach number range of the test was from 0.73 to 1.71.

Between Mach numbers of 0.73 and 0.90 the external-drag coefficient has a value of 0.017. The drag rise occurred at a Mach number of 0.93 and between Mach numbers of 1.05 and 1.71, the external-drag coefficient is constant at a value of 0.035. The transonic trim change was small for this model, with the center-of-gravity location at 6.56 percent of the mean aerodynamic chord.

INTRODUCTION

The test reported herein is the last phase of a program conducted by the Pilotless Aircraft Research Division to determine the low-lift drag of the Chance Vought XF8U-1 airplane. Tests of two early versions of this airplane are reported in reference 1 and a test of an area-rule version, with a faired inlet, is reported in reference 2. The entire program was conducted at the request of the Bureau of Aeronautics, Department of the Navy.

[redacted]

The Chance Vought XF8U-1 is a jet-propelled, swept-wing day fighter, with an all-movable horizontal tail and variable incidence wing. The duct inlet is an underslung scoop located near the nose and the fuselage cross section is developed on the supersonic-area-rule principle ($M = 1.2$).

This paper presents the minimum-drag data obtained from the flight test of a 0.11-scale rocket-boosted model of this configuration up to a Mach number near 1.7.

SYMBOLS

A	cross-sectional area, sq ft
a_l/g	longitudinal-accelerometer reading
a_n/g	normal-accelerometer reading
$\bar{c}$	mean aerodynamic chord, ft
C_c	chord-force coefficient, positive in rearward direction, $-\frac{a_l}{g}\left(\frac{W}{Sq}\right)$
C_D	drag coefficient, $\frac{\text{Drag}}{qS}$
C_N	normal-force coefficient, positive toward top of model, $\frac{a_n}{g}\left(\frac{W}{Sq}\right)$
H	total pressure, lb/sq ft
g	acceleration due to gravity, 32.2 ft/sec^2
γ	ratio of specific heats
l	length, ft
M	Mach number
m/m_o	ratio of mass flow through duct to mass flow through a stream tube of area equal to inlet-capture area under free-stream conditions
p	static pressure, lb/sq ft

q	dynamic pressure, lb/sq ft
R	Reynolds number based on mean aerodynamic chord of basic wing
r	radius, ft
S	model wing area (total wing without chord extensions), sq ft
V	velocity of model, ft/sec
W	weight of model, lb
x	station measured from nose, ft

Subscripts:

b	model base
c	choking-cup base
e	duct exit
i	duct inlet (capture)
o	free stream
tot	total drag
base	base drag
int	internal drag
ext	external drag

MODEL AND APPARATUS

Model

Figure 1 shows a three-view drawing of the model and the physical characteristics are presented in table I. The equivalent body of revolution and the normal-cross-sectional-area distribution are shown in figure 2, and a photograph of the model is presented in figure 3.

The model was similar in construction to the model described in reference 2, with the exception of the underslung scoop inlet and internal ducting. This ducting consisted of a single duct tube extending the length of the model with a choking cup installed at the duct exit in order to obtain a minimum section. A slotted total-pressure rake was installed at this minimum section to obtain data necessary to compute internal drag at supersonic speeds. A sketch of this installation is included in figure 1.

Because of the limited number of telemeter channels available for this test, the static pressure on the base of the choking cup was not measured. However, since the cup was similar in shape to the one discussed in reference 3 (on which the static base pressure of the cup was measured) these data were considered to be applicable to the test reported herein.

Four static-pressure orifices were located on the base of the model itself and manifolded together to give an average value of static pressure over the base of the model. These orifices were spaced 90° apart and located 0.5 inch from the edge of the base.

The model was boosted to a Mach number of 1.71 by two 6.25-inch ABL Deacon rocket motors. After the rocket motors had stopped thrusting, the model separated from the booster and the data presented herein were obtained during this coasting phase of the flight. Figure 4 is a photograph of the model-booster combination prior to launching.

Apparatus

Instrumentation of the model consisted of a telemeter system which measured data during the flight and transmitted it to a ground receiving station. The quantities measured for analysis were longitudinal and normal accelerations, base static pressure, and total pressures in free stream and at the duct exit.

A rawinsonde released at the time of firing recorded free-stream temperature, static pressure, and winds aloft. The velocity of the model and its position in space were determined by a CW Doppler radar set and NACA modified radar tracking unit, respectively.

ANALYSIS OF DATA

The drag and normal-force-coefficient data presented herein are based on the total wing area of the model without leading-edge extensions. Since the angle of attack of the model was small, the chord-force coefficients measured were considered to be constant with angle of attack and numerically equal to the minimum-drag coefficient for this test.

The Doppler radar set was also used to obtain total-drag data through a portion of the flight test. This method consists essentially of differentiating the velocity with respect to time and computing the drag from the acceleration thus obtained. Reference 1 discusses this method of drag reduction in more detail.

The external-drag coefficient $C_{D_{ext}}$ for the model was determined by subtracting the total-base-drag coefficient $C_{D_{base}}$ and the internal-drag coefficient $C_{D_{int}}$ from the faired curve of total-drag coefficient.

The total base drag of the model is the sum of the base drag of the choking cup and the base drag of the model itself. The base-pressure coefficient of the choking cup was assumed to be the same as that obtained and presented by reference 3, since the cups were similar in shape. Average values of static pressure over the base of the model (as obtained from the four manifolded static orifices) were used to obtain the base drag of the model. Base-drag coefficients were then computed by the following equation:

$$C_{D_{base}} = \left[\frac{-(p_b - p_o)(\text{Model base area})}{qS}\right] + \left[\frac{-(p_c - p_o)(\text{Choking-cup base area})}{qS}\right]$$

Reference 4 presents the method of data reduction used to determine the internal drag of the model. This method consists essentially of determining the loss in total momentum of the air flowing through the duct between free stream and exit. The equation used for internal-drag coefficient is as follows:

$$C_{D_{int}} = \frac{2A_e}{S}\left[\frac{m}{m_o}\left(\frac{A_i}{A_e}\right) - \frac{p_e}{p_o}\left(\frac{M_e}{M_o}\right)^2 - \left(\frac{p_e - p_o}{\gamma p_o M_o^2}\right)\right]$$

Because of the limited number of channels available for this test it was not possible to measure all of the quantities necessary at the duct exit. However, by choking the duct at this station a Mach number of 1.0 was assumed at the exit for free-stream Mach numbers greater than 1.0. The slotted total-pressure rake mounted near the choking section then supplied all the necessary conditions to satisfy the above equation at free-stream Mach numbers greater than 1.0.

Since the inlet was not operating at maximum mass-flow rates, there is some drag due to spillage included in the values of external drag presented herein. However, it is believed that the drag due to spillage was small because of the high mass-flow ratios of the test.

ACCURACY

A comparison between the two sources of Mach number from this test (telemeter and Doppler radar) in the range from 0.73 to 0.90 indicates agreement within 2 percent. From 1.05 to 1.71 the agreement between these two sets of Mach number values was better than 1 percent.

The accuracy of the total-drag values is indicated (by a comparison of the two sources of data) to be of the order of 0.0015 between Mach numbers of 1.03 and 1.71. At subsonic Mach numbers the drag values presented are believed to be correct within 0.0030. This order of agreement with comparative data at subsonic speeds is indicated by the comparisons presented in references 2 and 5.

RESULTS AND DISCUSSION

Figure 5 presents the Reynolds number range covered by this test. These values were based on the mean aerodynamic chord of the total wing.

Duct Performance

Shown in figure 6 are the mass-flow ratio m/m_o and total-pressure recovery H_e/H_o of the duct obtained during this test. By assuming that the static pressure at the duct exit was equal to the static pressure measured on the base of the model, it was possible to estimate values of m/m_o at Mach numbers less than 1.0. These estimates are shown by the dashed line in figure 6.

From $M = 0.73$ to $M = 0.98$, m/m_o has a constant value of 0.81. The mass-flow ratio increases from a value of 0.79 at $M = 1.01$ to 0.95 at $M = 1.71$.

Values of duct total-pressure recovery show a constant value of 1.0 from $M = 0.73$ to $M = 1.20$. This is followed by a decrease in H_e/H_o to a value of 0.90 at $M = 1.71$. Reference 6 presents the results of tests conducted in the Ames 6- by 6-foot supersonic tunnel with a model of this configuration with various nose and lip shapes. Total-pressure-recovery data have been taken from this reference for the applicable nose and lip shape and are presented at flight m/m_o for comparison in figure 6. These values show good agreement with the rocket-model data at Mach numbers of 0.9, 1.3, 1.5, and 1.7.

Trim Normal-Force Coefficient

Values of trim normal-force coefficient, $C_{N_{trim}}$, for the Mach range from 0.73 to 1.71 are shown in figure 7. These values were obtained with the model center of gravity located at 6.56 percent of the mean aerodynamic chord. The transonic trim change of the model with this center-of-gravity location was small, varying from $C_{N_{trim}} = -0.102$ at $M = 0.90$ to a value of $C_{N_{trim}} = -0.050$ at $M = 0.99$.

Total Drag

As mentioned previously in this paper, the total-drag coefficient $C_{D_{tot}}$ was determined during this flight test from telemeter values of longitudinal acceleration and from the Doppler radar unit. Values of $C_{D_{tot}}$ from both of these sources are plotted for a comparison in figure 8 and include internal- and base-drag coefficients. Although no drag data were obtained from the Doppler radar below $M = 1.03$ the agreement between the two sources of data from $M = 1.03$ to $M = 1.63$ is considered very good.

Internal and Base Drag

Figure 9 presents the variation of internal-drag coefficient $C_{D_{int}}$ and the base-drag coefficient $C_{D_{base}}$ with Mach number. The internal-drag coefficient is small, having a maximum value of 0.001 at $M = 1.71$. Below $M = 1.29$, the values of $C_{D_{int}}$ are within the accuracy of the measurements and are considered to be zero from $M = 0.73$ to $M = 1.29$. Base-drag-coefficient increases with increasing Mach number from a value of -0.0005 at $M = 0.93$ to 0.004 at $M = 1.33$. This is followed by a decrease in base drag to a value of 0.0025 at $M = 1.71$.

External Drag

The external-drag coefficient $C_{D_{ext}}$ $\left(C_{D_{ext}} = C_{D_{tot}} - C_{D_{int}} - C_{D_{base}}\right)$ is presented as a function of Mach number in figure 10. As discussed earlier in this paper, the effect of spillage drag on these values of $C_{D_{ext}}$ is considered to be negligible because of the high mass-flow ratios at which this test was conducted (fig. 6). From $M = 0.73$ to $M = 0.90$ the external-drag coefficient is constant at 0.017, and the drag rise $\left(\text{based on } \frac{dC_D}{dM} = 0.10\right)$ begins at $M = 0.93$. From $M = 1.05$ to $M = 1.71$ the drag level is 0.035.

CONCLUSIONS

From the flight test of a 0.11-scale rocket-boosted model of the Chance Vought XF8U-1 airplane at Mach numbers between 0.73 and 1.71 the following conclusions are indicated:

1. The external-drag coefficient $C_{D_{ext}}$ had a subsonic level of 0.017. The drag rise $\left(\text{based on } \frac{dC_D}{dM} = 0.10\right)$ occurred at a Mach number of 0.93. At supersonic Mach number the drag level was 0.035.

2. The transonic trim change was small for the model with the center-of-gravity location at 6.56 percent of the mean aerodynamic chord.

Langley Aeronautical Laboratory,
National Advisory Committee for Aeronautics,
Langley Field, Va., February 29, 1956.

Earl C. Hastings Jr.
Earl C. Hastings, Jr.
Aeronautical Research Scientist

Approved: Joseph A. Shortal
Joseph A. Shortal
Chief of Pilotless Aircraft Research Division

mr

REFERENCES

1. Blanchard, Willard S., Jr.: Minimum Drag of 0.11-Scale Rocket-Powered Models of the Chance Vought XF8U-1 Airplane, With and Without Nose Modifications, at Mach Numbers Between 0.85 and 1.30 - TED No. NACA DE 392. NACA RM SL54F17, Bur. Aero., 1954.

2. Hastings, Earl C., Jr.: Flight Determination of Minimum Drag of 0.11-Scale Rocket-Boosted Model of the Chance Vought XF8U-1 Airplane With Modified Fuselage Area Distribution and Faired Inlet at Mach Numbers From 0.82 to 1.68 - TED No. NACA DE 392. NACA RM SL55I27, Bur. Aero., 1955.

3. Mitcham, Grady L., and Blanchard, Willard S., Jr.: Low-lift Drag and Stability Data From Rocket Models of a Modified-Delta-Wing Airplane With and Without External Stores at Mach Numbers From 0.8 to 1.36. NACA RM L53A27, 1953.

4. Sears, R. I., and Merlet, C. F.: Flight Determination of the Drag and Pressure Recovery of an NACA 1-40-250 Nose Inlet at Mach Numbers From 0.9 to 1.8. NACA TN 3218, 1955. (Supersedes NACA RM L50L18.)

5. Purser, Paul E.: Comparison of Wind-Tunnel, Rocket, and Flight Drag Measurements for Eight Airplane Configurations at Mach Numbers Between 0.7 and 1.6. NACA RM L54F18, 1954.

6. Pfyl, Frank A.: An Investigation of the Effects of Nose and Lip Shapes for an Underslung Scoop Inlet at Mach Numbers From 0 to 1.9. NACA RM A55G13, 1955.

TABLE I

PHYSICAL CHARACTERISTICS OF 0.11-SCALE MODEL

Wing:	
Total area (excluding chord extensions), sq ft	4.53
Total area (including chord extensions), sq ft	4.66
Aspect ratio	3.40
Mean aerodynamic chord (excluding chord extensions), ft	1.29
Incidence angle, deg	-1
Dihedral angle, deg	-5
Sweepback (quarter-chord line), deg	42
Airfoil section at root, parallel to free-stream direction	NACA 65A006
Airfoil section at tip, parallel to free-stream direction	NACA 65A005
Taper ratio	0.25
Span, ft	3.92
Horizontal Tail:	
Total area, sq ft	1.14
Aspect ratio	3.5
Mean aerodynamic chord, ft	0.71
Incidence angle, deg	0
Dihedral angle, deg	5.4
Sweepback (quarter-chord line), deg	45
Airfoil section at root	NACA 65A006
Airfoil section at tip	NACA 65A004
Taper ratio	0.15
Span, ft	1.99
Vertical Tail (extended to horizontal-tail center line and not including dorsal fin):	
Area, sq ft	1.32
Aspect ratio	1.50
Mean aerodynamic chord, ft	1.05
Sweepback (quarter-chord line), deg	45
Airfoil section at water line 3.02 inches above fuselage reference line	NACA 65A006
Airfoil section at tip	NACA 65A004
Taper ratio	0.25
Span, ft	1.41
Duct:	
Inlet capture area, sq ft	0.051
Exit area, sq ft	0.041
Choking-cup base area, sq ft	0.010
Weight and Balance:	
Weight, lb	158.50
Wing loading, lb/sq ft	35.0
Center-of-gravity location, percent $\bar{c}$	6.56

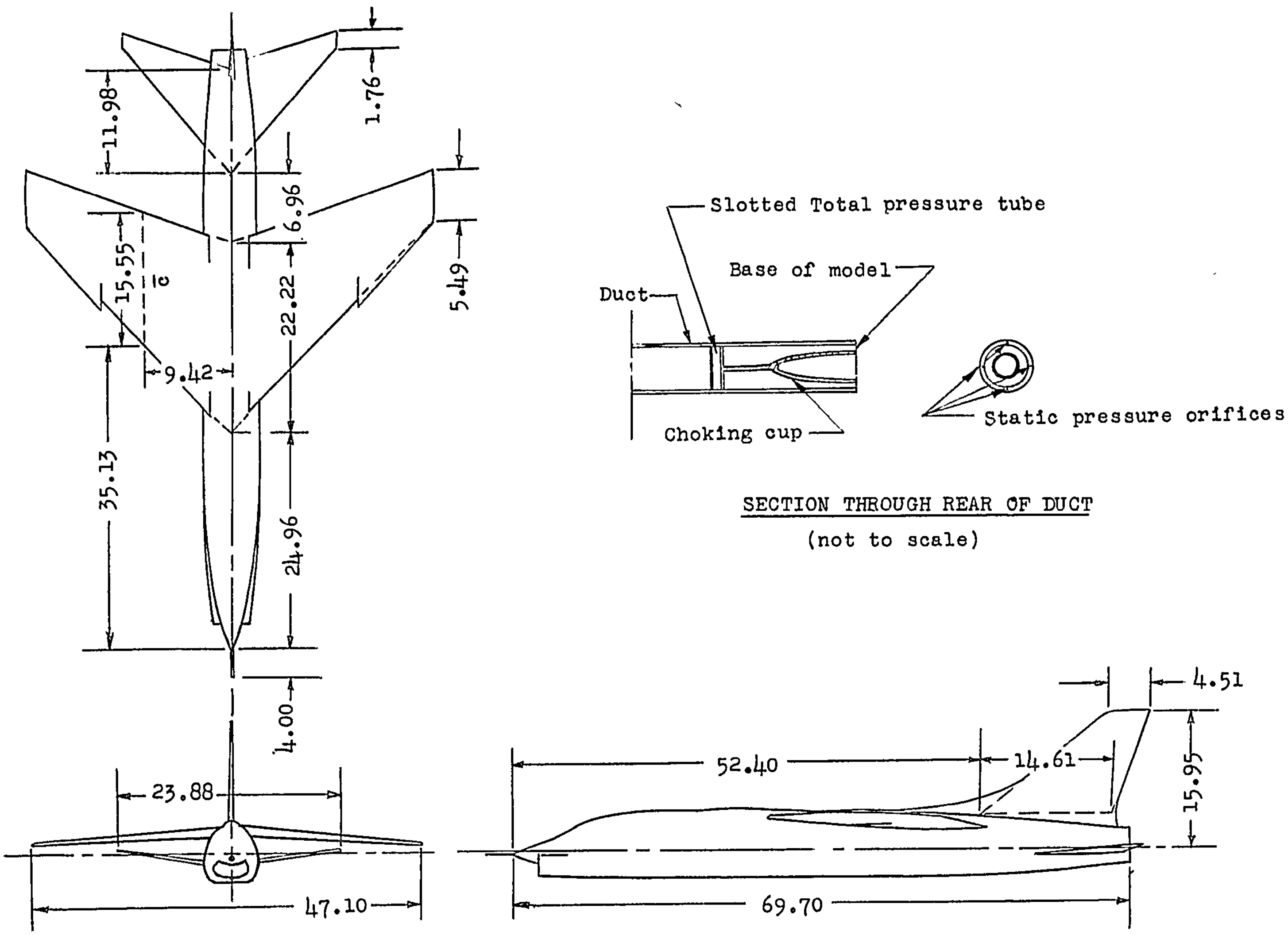

Figure 1.- Three-view drawing of model showing model design dimensions in inches.

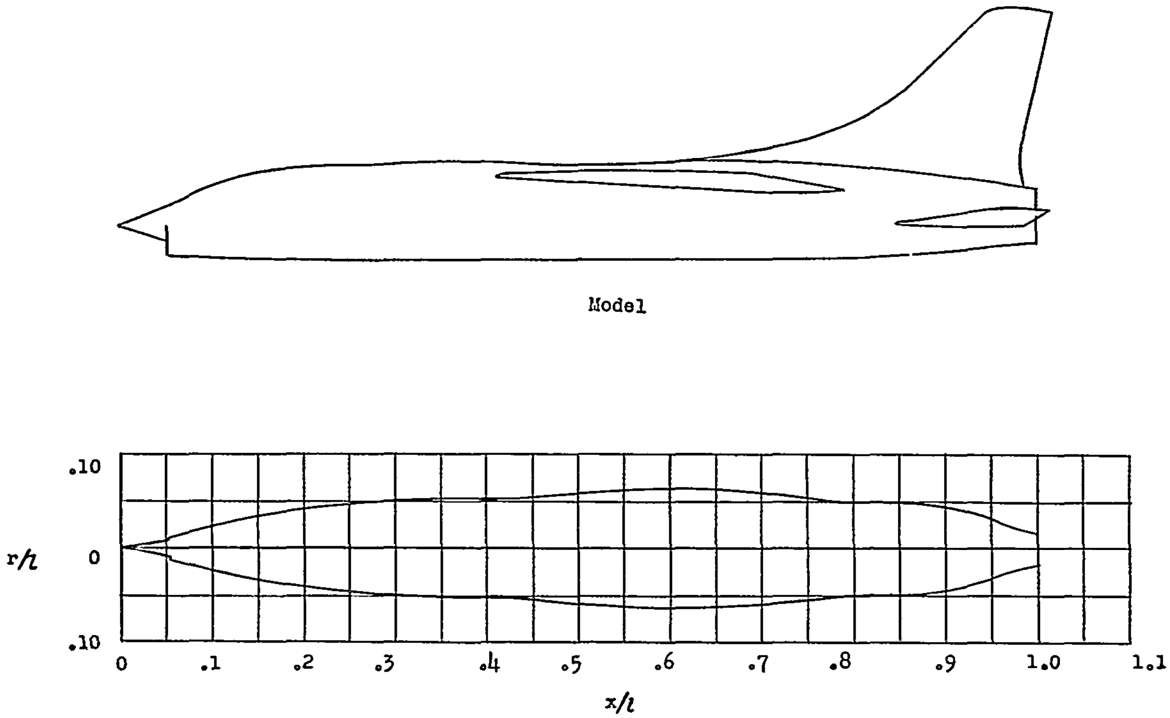

(a) Equivalent body of revolution.

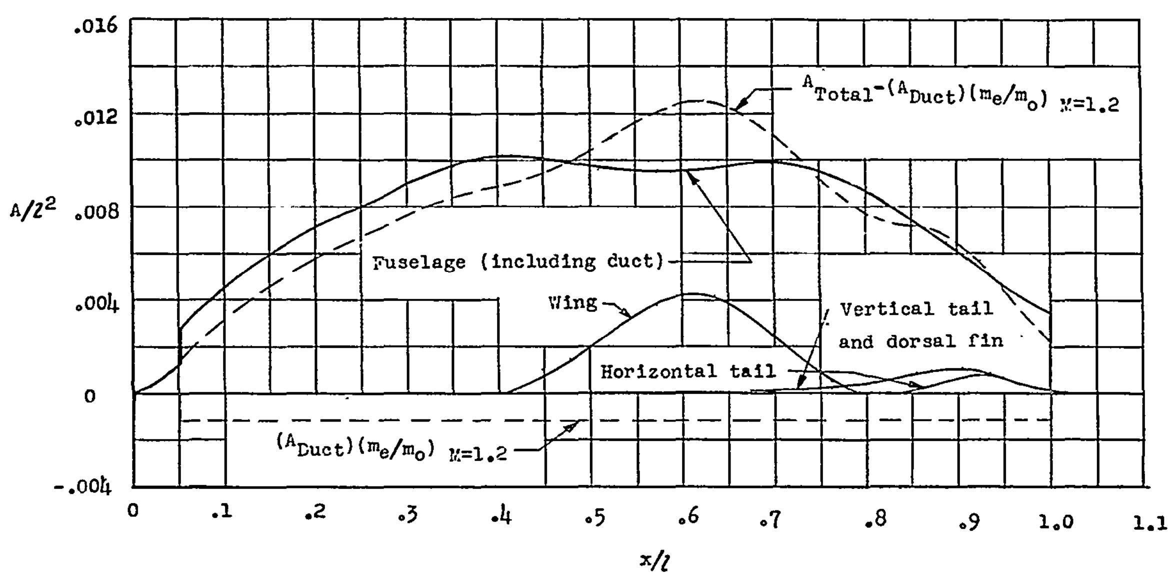

(b) Normal-cross-sectional-area distribution.

Figure 2.- Equivalent body of revolution and normal-cross-sectional-area distribution of the model.

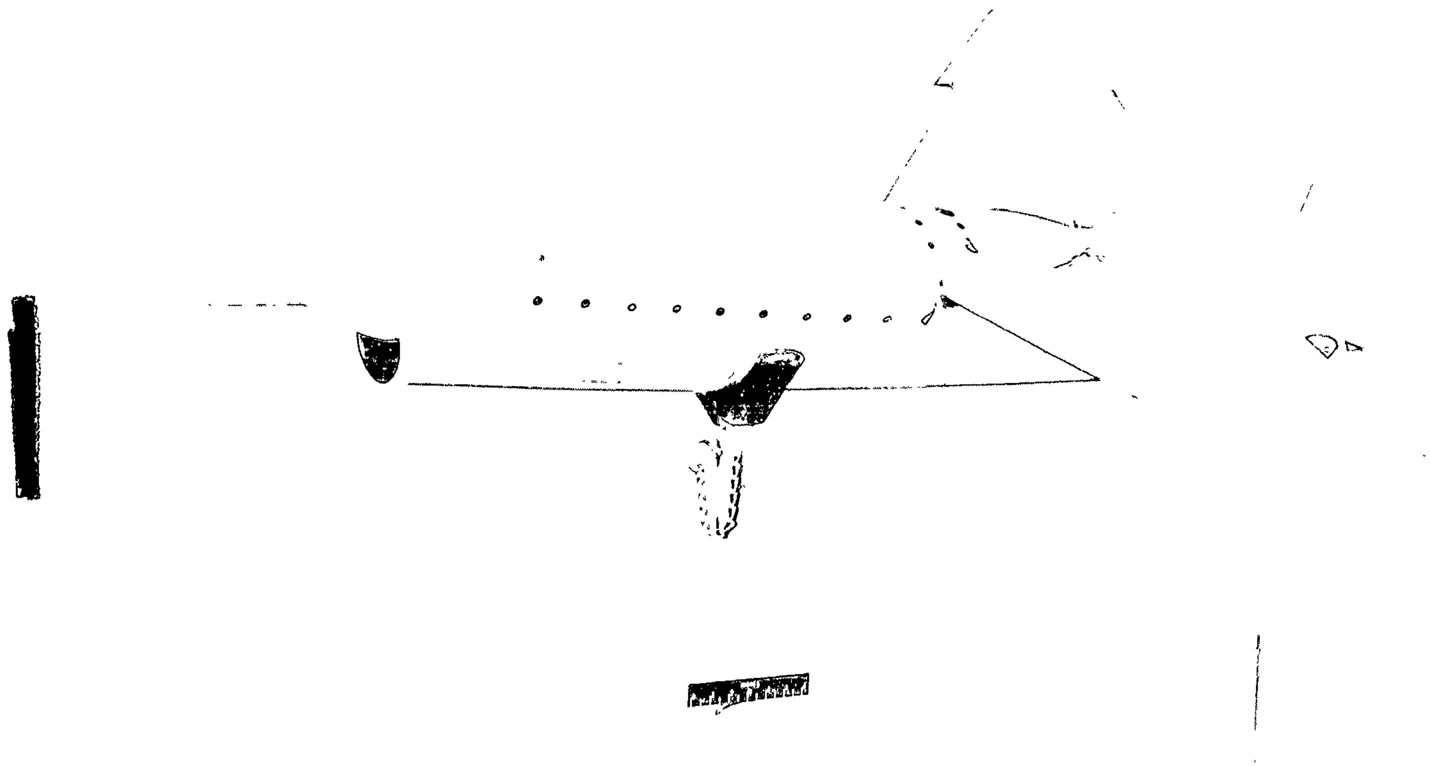

Figure 3.- Photograph of the model. L-90885.1

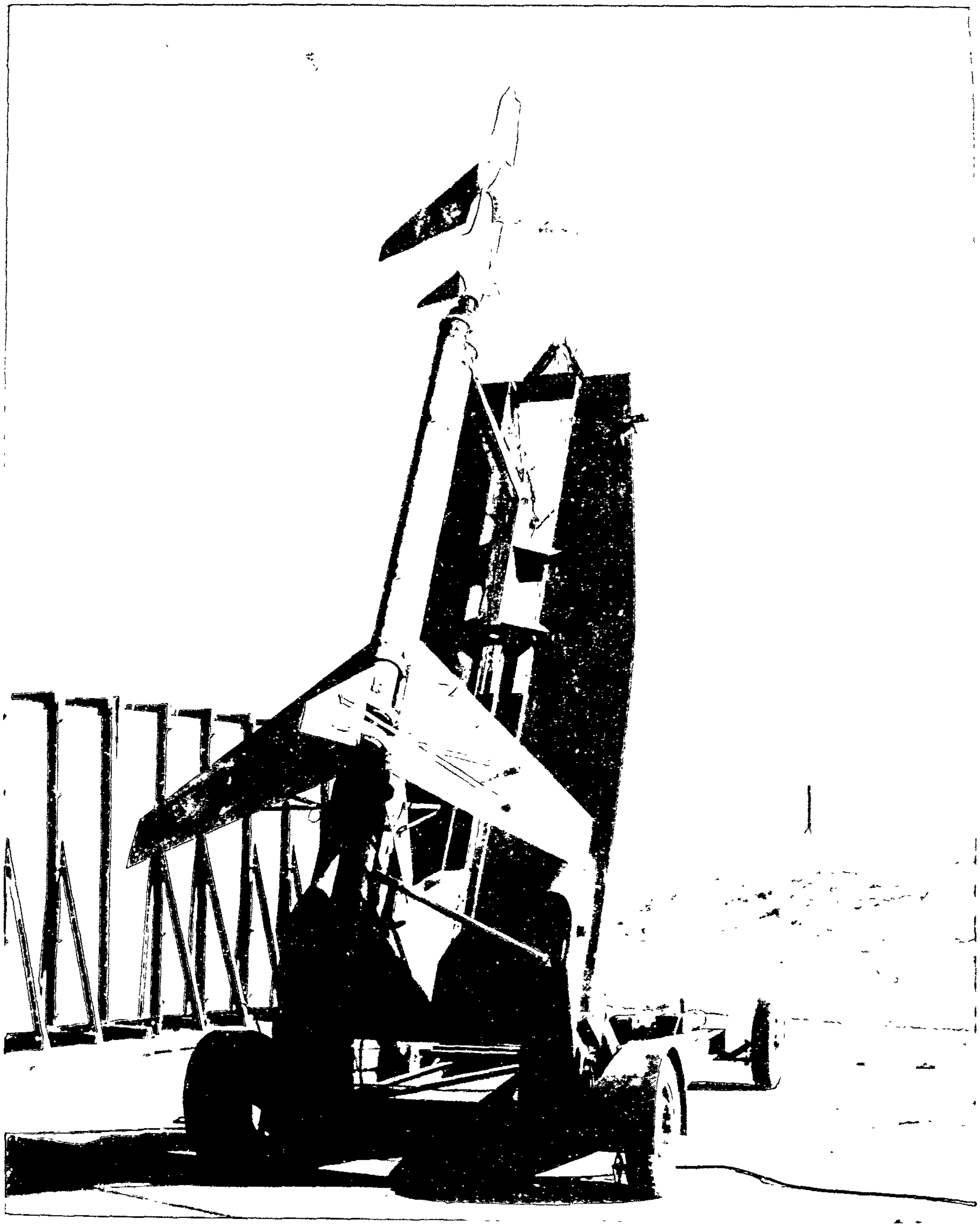

L-91899.1

Figure 4.- Photograph of the model-booster combination prior to launching.

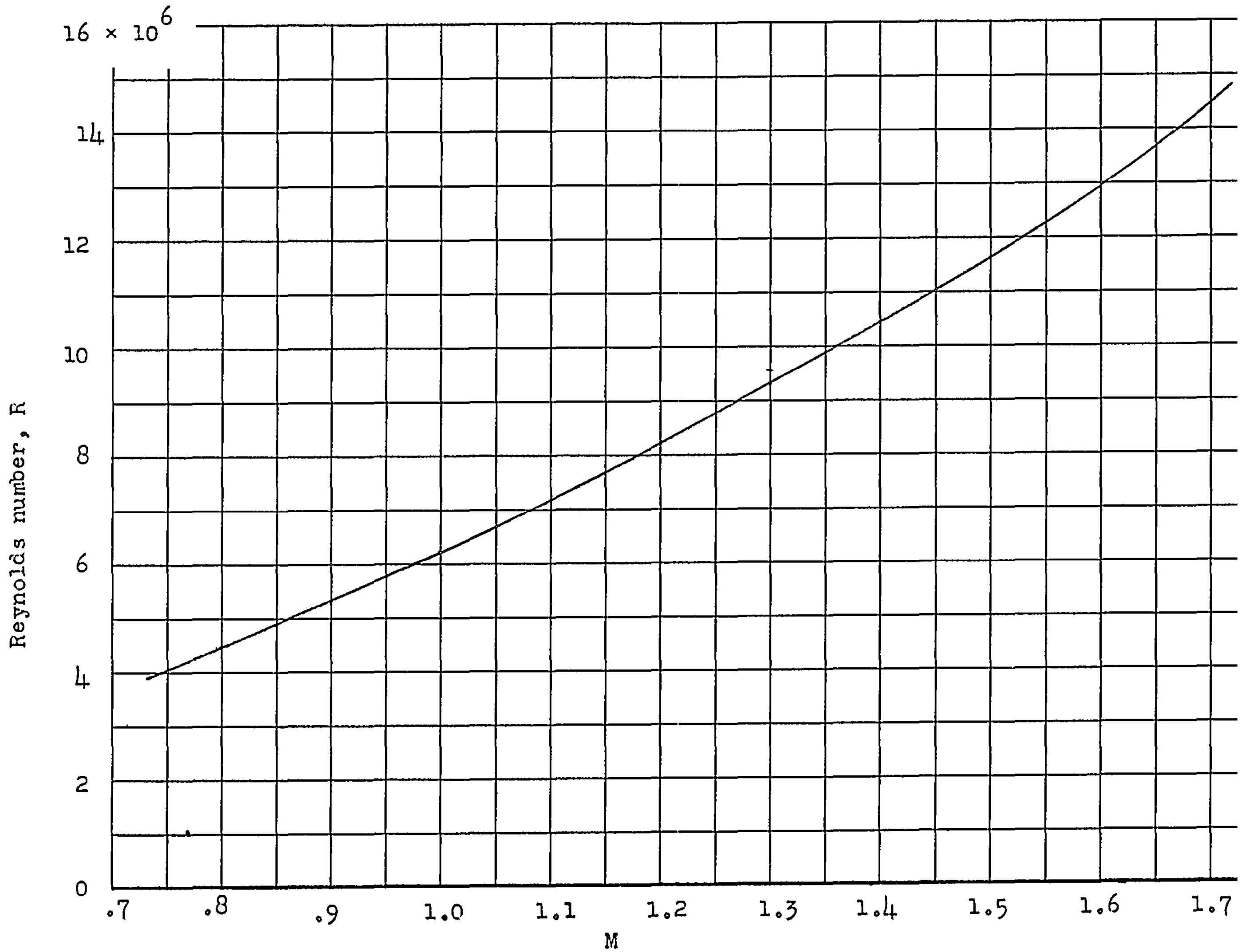

Figure 5.- Reynolds number as a function of Mach number.

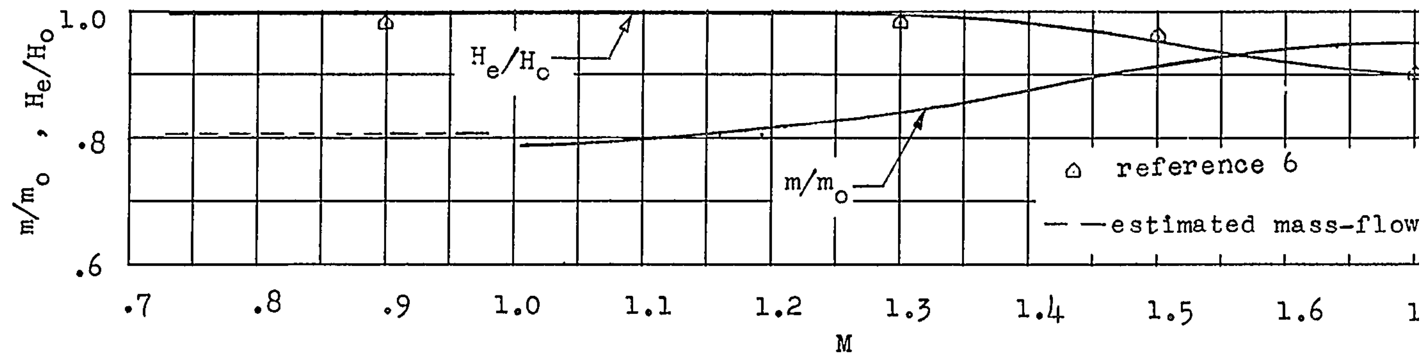

Figure 6.- Mass-flow ratio and total-pressure recovery.

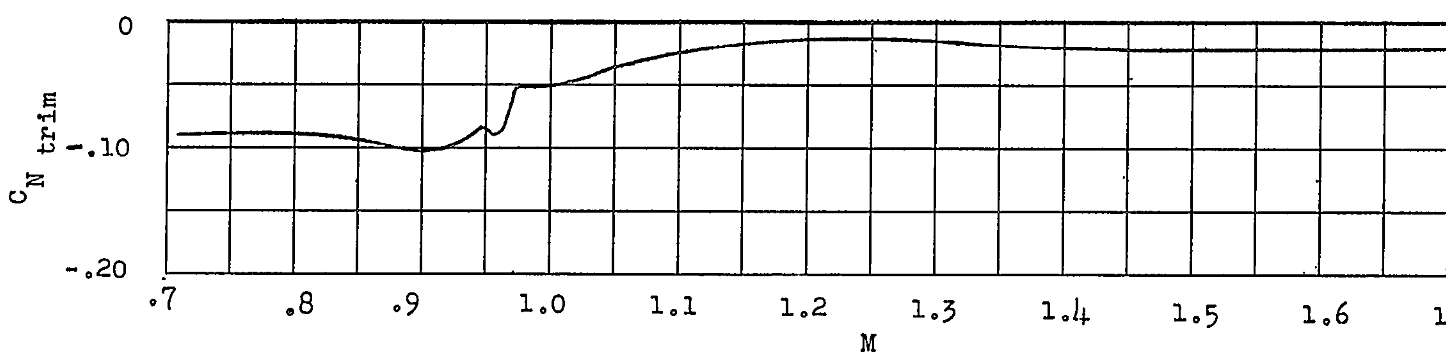

Figure 7.- Trim normal-force coefficient (c.g. location at 6.56 percent $\bar{c}$).

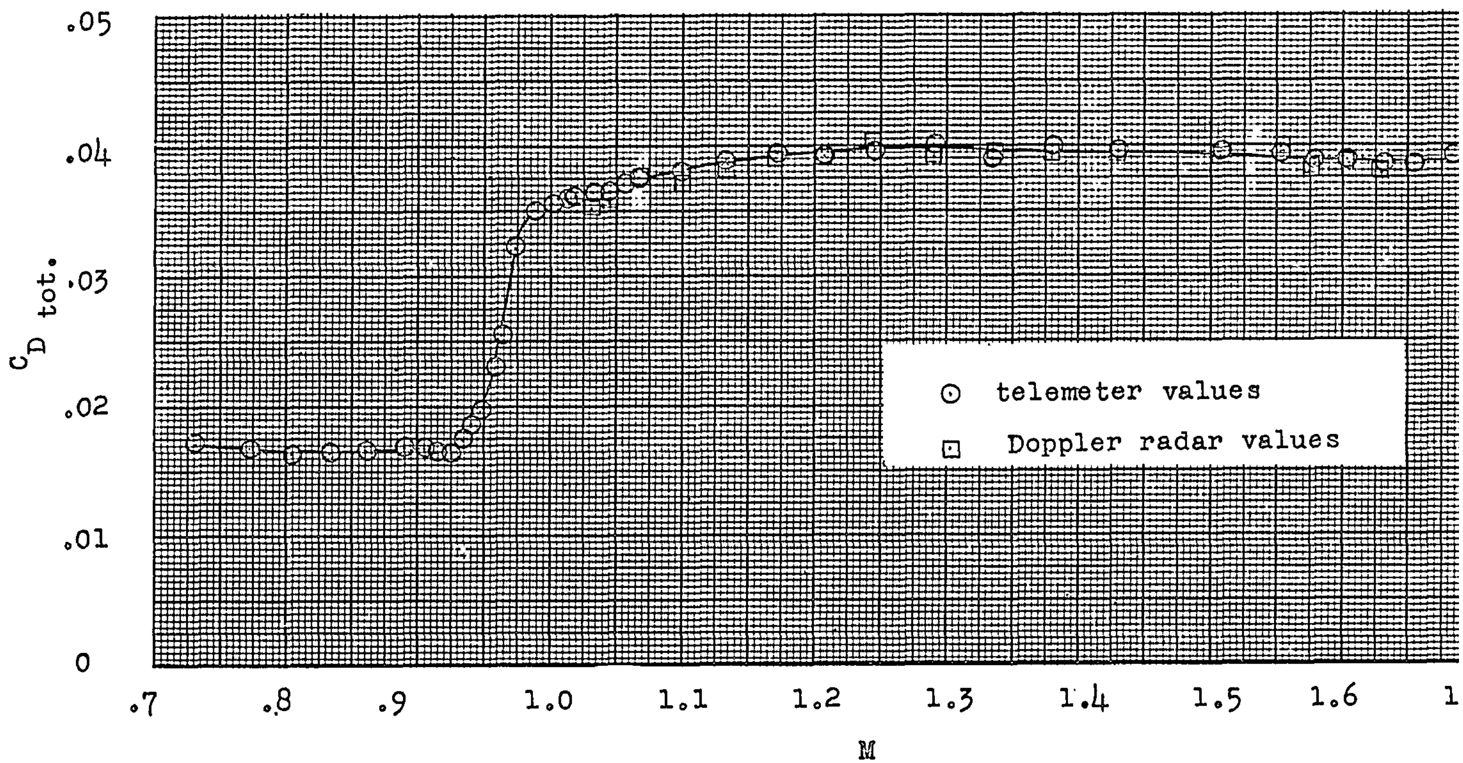

Figure 8.- Total-drag coefficient.

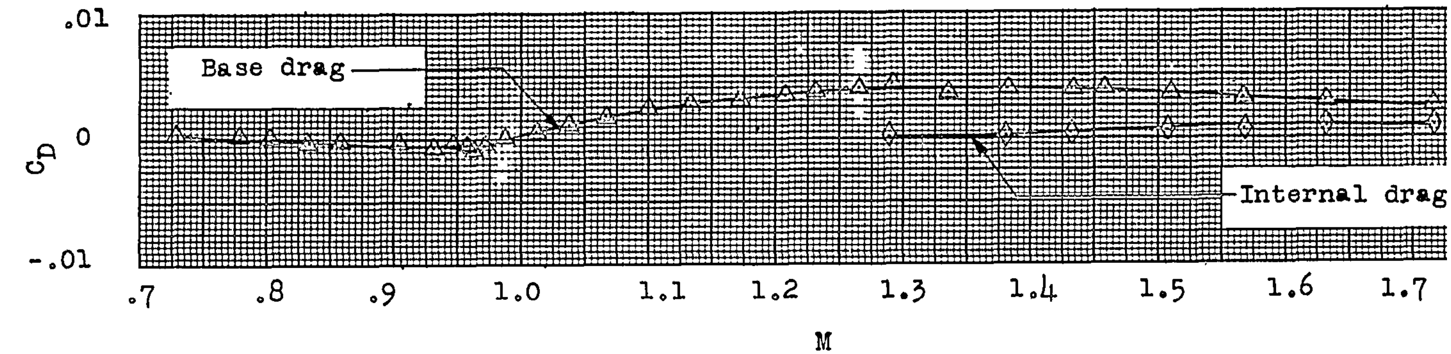

Figure 9.- Internal- and base-drag coefficients.

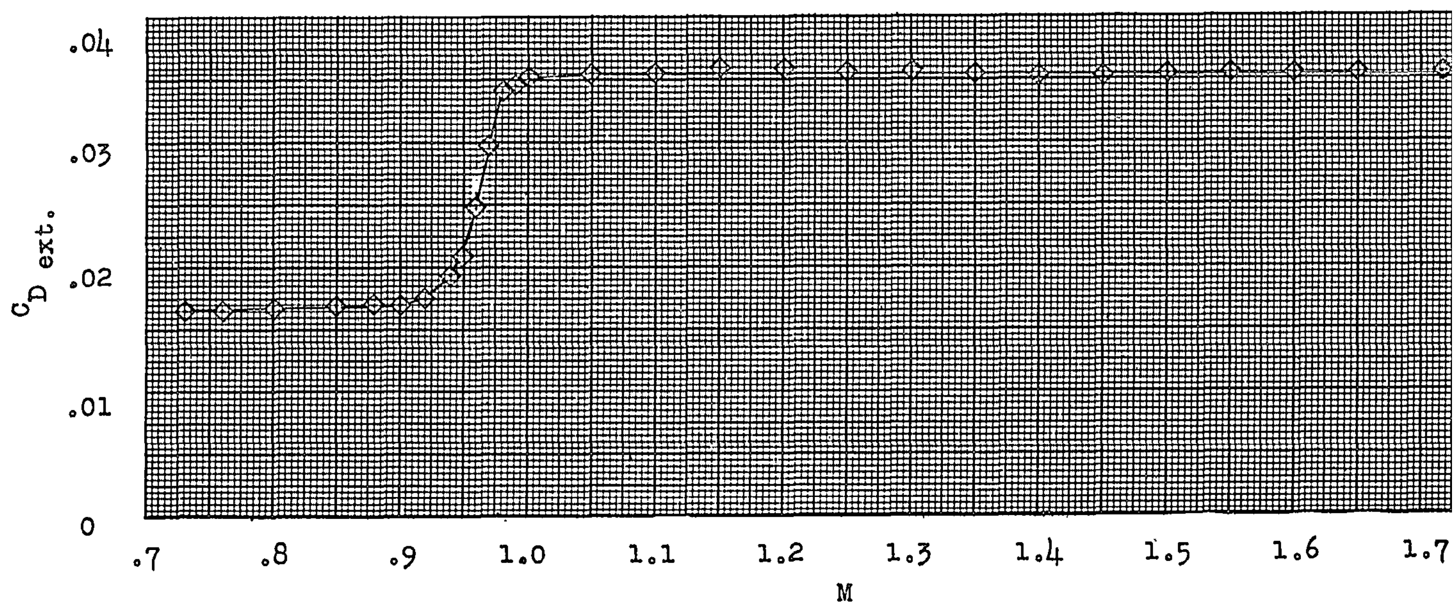

Figure 10.- External-drag coefficient.

UNCLASSIFIED

[redacted]

INDEX

Subject	Number
Air Inlets - Nose, Annular	1.4.1.2
Airplanes - Components in Combination	1.7.1.1
Airplanes - Specific Types	1.7.1.2

ABSTRACT

This paper presents the minimum drag of the Chance Vought XF8U-1 airplane as determined with a 0.11-scale rocket-boosted model in free flight. Minimum-drag data are presented between Mach numbers of 0.73 and 1.71.

[redacted]

UNCLASSIFIED

[redacted]

UNCLASSIFIED